

# Cerebrospinal fluid dynamics disorders

## Relationship to Alzheimer biomarkers and cognition

Jonathan Graff-Radford, MD, Jeffrey L. Gunter, PhD, David T. Jones, MD, Scott A. Przybelski, Christopher G. Schwarz, PhD, John Huston, III, MD, Val Lowe, MD, Benjamin D. Elder, MD, PhD, Mary M. Machulda, PhD, LP, Nathaniel B. Gunter, Ronald C. Petersen, MD, PhD, Kejal Kantarci, MD, Prashanthi Vemuri, PhD, Michelle M. Mielke, PhD, David S. Knopman, MD, Neill R. Graff-Radford, MD, and Clifford R. Jack, Jr., MD

### Correspondence

Dr. Graff-Radford  
graffradford.jonathan@mayo.edu

Neurology® 2019;93:e1-e10. doi:10.1212/WNL.0000000000008616

## Abstract

### Objective

To determine the frequency of high-convexity tight sulci (HCTS) in a population-based sample and whether the presence of HCTS and related features influenced participants' cognitive status and classification within the new Alzheimer-biomarker framework.

### Methods

We analyzed 684 participants  $\geq 50$  years of age who were enrolled in the prospective population-based Mayo Clinic Study of Aging and underwent structural MRI, amyloid PET imaging, and tau PET imaging. A fully automated machine-learning algorithm that had been developed previously in house was used to detect neuroimaging features of HCTS. On the basis of PET and MRI measures, participants were classified as having normal ( $A^-$ ) or abnormal ( $A^+$ ) amyloid, normal ( $T^-$ ) or abnormal ( $T^+$ ) tau, and normal ( $N^-$ ) or abnormal ( $N^+$ ) neurodegeneration. The neuropsychological battery assessed domain-specific and global cognitive scores. Gait speed also was assessed. Analyses were adjusted for age and sex.

### Results

Of 684 participants, 45 (6.6%) were classified with HCTS according to the automated algorithm. Patients with HCTS were older than patients without HCTS (mean [SD] 78.0 [8.3] vs 71.9 [10.8] years;  $p < 0.001$ ). More were cognitively impaired after age and sex adjustment (27% vs 9%;  $p = 0.005$ ). Amyloid PET status was similar with and without HCTS, but tau PET standard uptake value ratio (SUVR) was lower for those with HCTS after age and sex adjustment ( $p < 0.001$ ). Despite a lower tau SUVR, patients with HCTS had lower Alzheimer disease (AD) signature cortical thickness. With the amyloid-tau-neurodegeneration framework, HCTS was overrepresented in the  $T^-(N)^+$  group, regardless of amyloid status.

### Conclusion

The HCTS pattern represents a definable subgroup of non-AD pathophysiology (i.e.,  $T^-[N]^+$ ) that is associated with cognitive impairment. HCTS may confound clinical and biomarker interpretation in AD clinical trials.

From the Departments of Neurology (J.G.-R., D.T.J., R.C.P., D.S.K.), Radiology (J.L.G., C.G.S., J.H., V.L., N.B.G., K.K., P.V., C.R.J.), Health Sciences Research (S.A.P., M.M. Mielke), Neurologic Surgery (B.D.E.), and Psychiatry and Psychology (M.M. Machulda), Mayo Clinic, Rochester, MN; and Department of Neurology (N.R.G.-R.), Mayo Clinic, Jacksonville, FL.

Go to Neurology.org/N for full disclosures. Funding information and disclosures deemed relevant by the authors, if any, are provided at the end of the article.

## Glossary

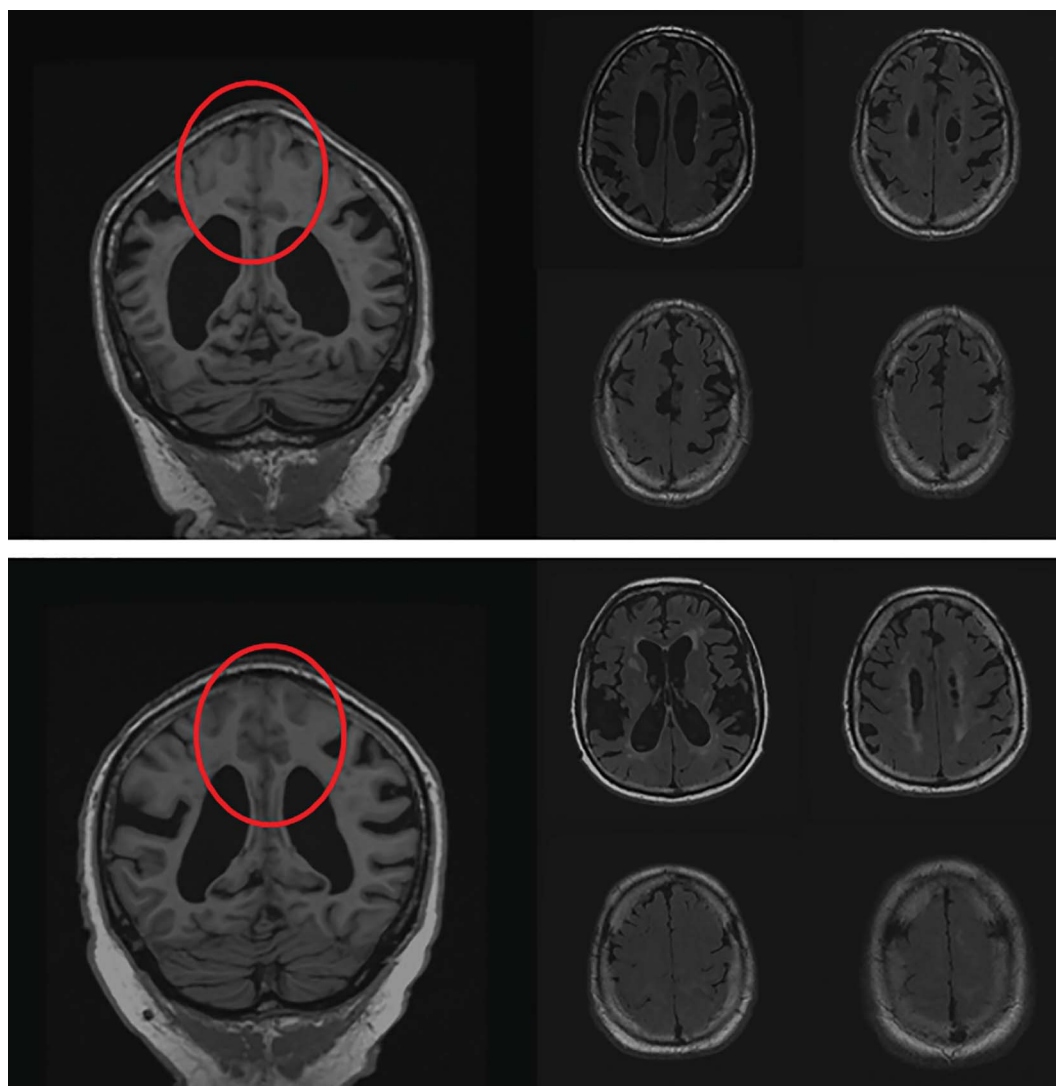
$A\beta_{42}$  =  $\beta$ -amyloid<sub>42</sub>; AD = Alzheimer disease; AT(N) = amyloid-tau-neurodegeneration; CDD = CSF dynamics disorder; DESH = disproportionately enlarged subarachnoid space hydrocephalus; FLAIR = fluid-attenuated inversion recovery; HCTS = high-convexity tight sulci; MCALT = Mayo Clinic Adult Lifespan Template; MCSA = Mayo Clinic Study of Aging; MPRAGE = magnetization-prepared rapid gradient-echo; NPH = normal-pressure hydrocephalus; PiB = Pittsburgh compound B; SUVR = standard uptake value ratio.

The combination of high-convexity tight sulci (HCTS), defined as compression of sulci at the vertex (figure 1), enlarged CSF spaces in the Sylvian fissure, and ventriculomegaly, is an established neuroimaging phenotype of a CSF dynamics disorder (CDD) called disproportionately enlarged subarachnoid space hydrocephalus (DESH).<sup>1</sup> Although DESH was originally identified in individuals with symptomatic, normal-pressure hydrocephalus (NPH), recent population studies suggest that features of DESH are more common with advancing age and occur more

frequently among persons without obvious symptoms than previously believed.<sup>2,3</sup>

We previously developed an automated algorithm to detect HCTS in MRIs.<sup>4</sup> In this study, the HCTS is used as an indirect marker of a CDD. Unlike the other features of DESH (ventriculomegaly and widened sylvian fissure), which can be seen in neurodegenerative disease, compression of the sulci distinguishes HCTS from a neurodegenerative process such as AD,<sup>5</sup> which would result in widening of the sulci.

**Figure 1** Examples of high-convexity tight sulci (circled red areas) from individual participants



Furthermore, when HCTS occurs in NPH, it is often associated with improvement in symptoms after ventricular shunting.<sup>6</sup> This supports the assumption that HCTS is indeed a disorder of CSF dynamics.

Whether HCTS influences neurodegenerative biomarkers is of particular importance, given the new research framework for Alzheimer disease (AD) published by the National Institute on Aging and Alzheimer's Association,<sup>7</sup> that defines AD on the basis of both abnormal amyloid and tau biomarkers. The amyloid-tau-neurodegeneration [AT(N)] biomarker scheme classifies participants as having normal (A<sup>-</sup>) or abnormal (A<sup>+</sup>) amyloid, normal (T<sup>-</sup>) or abnormal (T<sup>+</sup>) tau, and normal (N<sup>-</sup>) or abnormal (N<sup>+</sup>) neurodegeneration.

In HCTS, the ventricles and Sylvian fissures can enlarge and mimic atrophy (i.e., neurodegeneration). We therefore hypothesized that this pattern could be overrepresented among persons with normal tau levels and abnormal neurodegeneration (T<sup>-</sup>[N]<sup>+</sup>). An additional objective therefore was to determine the frequency of HCTS and to categorize persons with the HCTS pattern of structural imaging abnormalities within the AT(N) biomarker framework.<sup>7</sup>

## Methods

### Participants

The Mayo Clinic Study of Aging (MCSA) is a population-based study that focuses on cognitive decline; details of the study design have been published previously.<sup>8</sup> Using an age- and sex-stratified random sampling design, the MCSA initially enumerated residents of Olmsted County, Minnesota, who were 70 to 89 years of age on October 1, 2004, with the Rochester Epidemiology Project medical records linkage system.<sup>9</sup> In 2012, the age range was expanded to enumerate and sample Olmsted residents 50 to 69 years of age. For the current study, MCSA participants ≥50 years of age were included if they had undergone structural MRI, amyloid PET imaging, and tau PET imaging.

### Cognitive evaluation

The neuropsychological assessment battery included 9 tests covering 4 cognitive domains: (1) memory (Wechsler Memory Scale–Revised [Logical Memory II and Visual Reproduction II Tests]; Auditory-Verbal Learning Test [delayed-recall trial]), (2) attention-executive function (Wechsler Adult Intelligence Scale–Revised [Trail Making Test part B, digit symbol subtest]), (3) language (Boston Naming Test [fluency category]), and (4) visuospatial skills (Wechsler Adult Intelligence Scale–Revised [Block Design and Picture Completion subtests]). In addition, raw test scores were averaged and scaled to create a domain *z* score to facilitate comparisons across domains. The *z* scores from the 4 domains were averaged and scaled to calculate a global cognitive *z* score.<sup>8</sup>

Participant evaluations included a review of the medical history and an interview by a study coordinator. A physician performed a medical history review, mental status examination, and neurologic examination. A neuropsychological examination was also performed. Participants were then classified as cognitively impaired or unimpaired by a consensus panel consisting of the examining physician, the study coordinator, and a neuropsychologist, as previously described.<sup>8</sup> Those with mild cognitive impairment or dementia were considered cognitively impaired. The diagnosis of cognitively unimpaired was established by the use previously published criteria.<sup>10,11</sup>

### Other covariates

Demographics (age, sex, and years of education) were assessed by interview and electronic health record review. A nurse abstracted clinical data from the medical records linkage system.<sup>9</sup> APOE status (ε4 carrier) was assessed at baseline.

Gait velocity (measured in meters per second) was assessed over 7.62 m (25 ft) at a self-selected pace. The full details of the gait evaluation have been previously published.<sup>12</sup>

## Neuroimaging

### Magnetic resonance imaging

Magnetization-prepared rapid gradient-echo (MPRAGE) and fluid-attenuated inversion recovery (FLAIR) images were acquired as part of the standard MCSA MRI protocol. Consistent imaging parameters were used throughout, and imaging was performed with 3T GE MRI scanners (GE Healthcare, Chicago, IL). Complete details of the acquisitions can be found elsewhere.<sup>13</sup>

The FLAIR MRI was used to ascertain vascular disease by assessing subcortical infarcts, cortical infarcts, and white matter hyperintensity load. All brain infarctions were assessed by a trained image analyst and confirmed by a vascular neurologist or radiologist (K.K., J.G.-R., C.R.J.) blinded to all clinical information.<sup>14</sup> White matter hyperintensity load was assessed with a semiautomated FLAIR algorithm, as previously described.<sup>15</sup>

MPRAGE images were analyzed with probabilistic segmentation using SPM12 with the Mayo Clinic Adult Lifespan Template (MCALT)<sup>16</sup> population-optimized priors and settings ([nitrc.org/projects/mcalt/](http://nitrc.org/projects/mcalt/)), and deformations were calculated by mapping the template grayscale image to each subject scan using the Advanced Normalization Tools<sup>17</sup> toolkit. Two atlas parcellations, one with 122 tissue regions (MCALT\_AD122) and another with 123 named sulcal regions (adapted from BrainVISA [[brainvisa.info](http://brainvisa.info)]), were propagated from MCALT coordinates to subject space.

Cortical thickness was estimated with FreeSurfer 5.3.<sup>18</sup> Average cortical thickness measures in the entorhinal, fusiform, parahippocampal, midtemporal, inferior-temporal, and angular gyrus regions of interest were combined to create an AD

signature measurement. An abnormal AD signature cortical thickness ( $N^+$ ) was defined as  $<2.68$  mm.<sup>19</sup>

Using the segmentation procedures described in the following section, we calculated ventricular volumes and normalized them to total intracranial volume with FreeSurfer 5.3.

## Measuring HCTS

We have developed a fully automated imaging pipeline to detect HCTS that is described in prior work.<sup>4</sup> In brief, the algorithm begins with the SPM12 CSF segmentation output probability in each sulcal region that is normalized to total intracranial volume. In order to train the algorithm, manual grading for the presence of high-convexity tightness was previously completed by an expert, and this information was used as the standard against which a machine-learning algorithm was trained.<sup>4</sup> CSF regions relevant to predicting the presence of high-convexity tightness were chosen by an area under the receiver operating characteristic curve analysis. A support vector machine model was then trained on the regions selected. Using the model, the methodology classified scans for HCTS with an area under the receiver operating characteristic curve  $>0.96$  with respect to the expert evaluations.<sup>4</sup> Figure 1 provides an example of 2 cases of ventriculomegaly and HCTS from our cohort. This machine-learning pipeline was previously validated on a dataset separate from the training data set.<sup>4</sup>

## Validation study

Although the automated HCTS detection algorithm was previously validated,<sup>4</sup> we performed an independent validation for the present study. We randomly selected 10 participants with an HCTS score  $>1$ , 10 participants with an HCTS score close to the overall median, and 10 participants without HCTS from the present cohort. These images were visually graded for presence or absence of an HCTS by a board-certified neuroradiologist (J.H.) blinded to the machine-learning categorization. The visual grading served as the gold standard for the independent validation study.

## Positron emission tomography

Amyloid PET imaging was performed with Pittsburgh compound B (PiB), and tau PET was performed with AV1451, with precursor supplied by Avid Radiopharmaceuticals (Philadelphia, PA). Details of PET acquisition have been published previously.<sup>20,21</sup> Participant PET scans were aligned to their corresponding MPRAGE images by using a rigid transformation computed with SPM12 and combined with the Advanced Normalization Tools MCALT-to-subject warps to place atlases in PET image space. The full details of amyloid and tau PET acquisition have been published elsewhere.<sup>22</sup> An abnormal amyloid level ( $A^+$ ) was defined as a PiB standard uptake value ratio (SUVR)  $>1.48$ . An abnormal tau ( $T^+$ ) was defined as a tau SUVR  $>1.25$ .<sup>23</sup>

## Statistical analysis

Continuous variables were compared with  $t$  tests, and differences in proportions were compared with  $\chi^2$  tests.

Additional testing was adjusted for age and sex. The tests for continuous variables were performed with analysis of covariance models, and categorical variables were assessed with logistic regression models. Values of  $p < 0.05$  were considered significant.

## Sensitivity analysis

As shown later, the cerebrovascular disease burden was increased among participants with HCTS. We therefore performed a sensitivity analysis evaluating associations with HCTS in only those without infarcts.

## Standard protocol approvals, registrations, and patient consents

The Mayo Clinic Institutional Review Board and the Olmsted Medical Center Institutional Review Board approved all study protocols. Written informed consent was obtained from all participants. The reporting of this study is in compliance with Strengthening the Reporting of Observational Studies in Epidemiology guidelines.<sup>24</sup>

## Data availability

Data from the MCSA, including data from this study, are available on request.

# Results

## Characteristics of participants

We included 684 participants in the study. Forty-five (6.6%) were classified as having HCTS. The demographic characteristics of the participants with and without HCTS are listed in table 1. Compared with those who did not have HCTS, those with HCTS were older (mean [SD] age, 78.0 [8.3] vs 71.9 [10.8] years;  $p < 0.001$ ) and more often cognitively impaired after adjustment for age.

## Neuroimaging

Figure 2 shows MRI features characteristic of HCTS. Table 2 compares the neuroimaging characteristics of those with and those without HCTS. The HCTS group had larger ventricles ( $p < 0.001$ ) and a lower tau SUVR ( $p < 0.001$ ), despite being older. There was no difference between the groups in PiB SUVR ( $p = 0.52$ ). The HCTS group also had lower AD signature cortical thickness ( $p = 0.02$ ), greater white matter hyperintensity volume ( $p < 0.001$ ), and more infarctions ( $p = 0.03$ ).

We next determined the difference in AT(N) biomarker profiles between the 2 groups. Because amyloid PET SUVR did not differ between the 2 groups, we did not differentiate between participants who were  $A^+$  or  $A^-$  in the comparison (table 3). The HCTS group was more commonly  $T^-$  and ( $N$ )<sup>+</sup> (56%) compared with the no-HCTS group (23%) ( $p < 0.001$ ). The AT(N) biomarker profiles of the individual patients are reported in table e-1 (available from Dryad, doi.org/10.5061/dryad.mn176dr).



**Table 1** Characteristics of participants, stratified by the presence of CDD

Characteristic	No HCTS (n = 639)	HCTS > 1 (n = 45)	p Value	Adjusted p value <sup>a</sup>
Male, n (%)	350 (55)	26 (58)	0.70	—
Age, mean (SD), y	71.9 (10.8)	78.0 (8.3)	<0.001	—
APOE ε4 carrier, n (%)	177 (29)	18 (40)	0.11	0.10
Education, mean (SD), y	14.8 (2.6)	14.4 (2.7)	0.33	0.61
Cognitively impaired, n (%)	59 (9)	12 (27)	<0.001	0.005

Abbreviations: CDD = CSF dynamics disorder; HCTS = high-convexity tight sulci.  
<sup>a</sup> Adjusted for age and sex.

### Cognitive testing and gait evaluation

Table 4 summarizes the cognitive profile and gait speed by HCTS status. The groups had similar scores for memory and visual-spatial function, but the HCTS group had lower scores in the attention ( $p = 0.02$ ) and language domains (0.002) after adjustment for age. Gait velocity was slower in the HCTS group ( $p = 0.34$ ), but the differences were not significant after adjustment for age and sex.

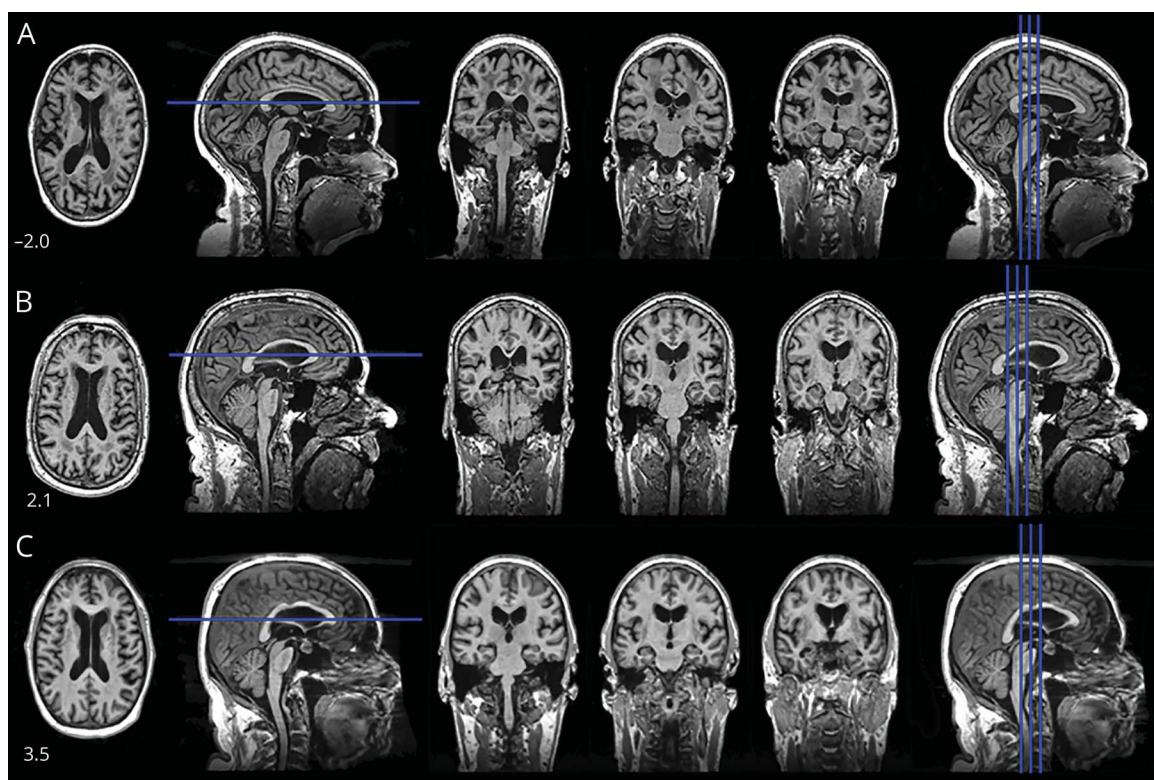
### Independent validation study

Of 30 images reviewed, the expert visual rater graded 8 as having an HCTS and 22 as not having an HCTS. The

machine-learning method was 8 of 8 sensitive for the cases visually graded as positive and 20 of 22 specific for cases visually rated as negative or 100% sensitive and 90.9% specific relative to the expert visual grading. There were 2 cases that the algorithm classified as HCTS that the rater did not rate as HCTS.

### Sensitivity analysis

Participants with HCTS were more likely to have cerebrovascular disease than those without an HCTS. Therefore, we performed a secondary analysis among participants without infarcts. The findings remained unchanged. Those with

**Figure 2** Images from 3 participants (A, B, C) are shown

The number in the lower left corner is the score from the high-convexity tightness classifier (positive values = tighter). Top row represents those without high-convexity tight sulci. Overall, the CSF spaces are increasingly larger, with the exceptions of the high convexity and on the midline.

**Table 2** Neuroimaging characteristics, stratified by the presence of CDD

Characteristic	No HCTS (n = 639)	HCTS > 1 (n = 45)	p Value	Adjusted p value <sup>a</sup>
PiB SUVR, mean (SD)	1.58 (0.41)	1.65 (0.46)	0.25	0.52
Tau SUVR, mean (SD)	1.20 (0.13)	1.17 (0.10)	0.048	<0.001
FDG SUVR, mean (SD)	1.54 (0.14)	1.47 (0.17)	0.02	0.16
Cortical thickness, mean (SD), mm	2.70 (0.16)	2.60 (0.12)	<0.001	0.02
WMH volume, mean (SD), cm <sup>3</sup>	13.8 (15.1)	38.6 (30.3)	<0.001	<0.001
Ventricle volume, mean (SD), cm <sup>3</sup>	34.9 (17.9)	76.4 (23.9)	<0.001	<0.001
<b>Infarction present, n (%)</b>				
Any type	118 (19)	18 (41)	<0.001	0.03
Cortical	40 (6)	5 (11)	0.20	0.57
Subcortical	94 (15)	16 (36)	<0.001	0.01

Abbreviations: CDD = CSF dynamics disorder; FDG = fludeoxyglucose; HCTS = high-convexity tight sulci; PiB = Pittsburgh compound B; SUVR = standard uptake value ratio; WMH = white matter hyperintensities.

<sup>a</sup> Adjusted for age and sex. PiB, tau, the variables associated with WMH, and ventricle volume were log-transformed before statistical testing because of skewed data.

HCTS were more likely to have abnormal AD signature cortical thickness 69% (n = 18) compared to those without HCTS 36% (n = 179) ( $p = 0.037$ ) after adjustment for age and sex. Participants with HCTS were similarly over-represented among the T-N+ (65%) vs (22%) group. Participants with HCTS had lower scores in the language domain after adjustment for age ( $p = 0.022$ ). The difference in the attention domain was no longer significant after the exclusion of individuals with infarcts.

## Discussion

In the MCSA, of the participants  $\geq 50$  years of age who underwent brain MRI and PET imaging,  $\approx 6.6\%$  were classified as having HCTS. Those with HCTS were older, and a greater

proportion had cognitive impairment, even after adjustment for age. In addition, the presence of HCTS appears to have an important influence on AD biomarker-profile classifications (i.e., AT[N]) currently being used in research and clinical trials.<sup>7</sup>

Those with HCTS more commonly were characterized as (N)<sup>+</sup> on the basis of abnormal AD signature cortical thickness. Despite their older age, participants with HCTS had a lower tau burden (more often T<sup>-</sup>), indicating that the abnormal AD signature cortical thickness could not be explained by tauopathy. Whether the abnormal AD signature thickness is due to nonatrophy effects (e.g., compression, rather than destruction, of tissue) or whether it truly represents decreased cortical thickness is an important area of future investigation. The AD signature thickness region included areas in the basal-medial temporal lobe, not the parietal lobe, so the decreased

**Table 3** AT(N) biomarker groupings, stratified by the presence of CDD

Characteristic <sup>a</sup>	No HCTS (n = 639)	HCTS > 1 (n = 45)	p Value	Adjusted p value <sup>b</sup>
A <sup>+</sup> T <sup>-</sup> (N) <sup>-</sup> , n (%)	288 (45)	11 (24)	<0.001	—
A <sup>+</sup> T <sup>-</sup> (N) <sup>+</sup> , n (%)	149 (23)	25 (56)	—	—
A <sup>+</sup> T <sup>+</sup> (N) <sup>-</sup> , n (%)	87 (14)	0 (0)	—	—
A <sup>+</sup> T <sup>+</sup> (N) <sup>+</sup> , n (%)	110 (17)	9 (20)	—	—
Abnormal PiB SUVR, n (%)	235 (37)	21 (47)	0.19	0.79
Abnormal tau SUVR, n (%)	160 (25)	8 (18)	0.27	0.04
Abnormal cortical thickness, n (%)	259 (41)	34 (76)	<0.001	0.007

Abbreviations: AT(N) = amyloid-tau-neurodegeneration; CDD = CSF dynamics disorder; HCTS = high-convexity tight sulci; PiB = Pittsburgh compound B; SUVR = standard uptake value ratio.

<sup>a</sup> Amyloid SUVR did not differ between the 2 groups; therefore, comparisons did not differentiate between participants who were A<sup>+</sup> or A<sup>-</sup>.

<sup>b</sup> Adjusted for age and sex.

**Table 4** Cognitive and gait differences, stratified by the presence of CDD

Characteristic <sup>a</sup>	No HCTS (n = 639)	HCTS > 1 (n = 45)	p Value	Adjusted p value <sup>b</sup>
Velocity (gait), mean (SD)	113.8 (22.6)	103.9 (20.9)	0.007	0.34
Global, mean (SD)	0.24 (1.19)	-0.32 (1.30)	0.005	0.20
Memory, mean (SD)	0.21 (1.24)	-0.12 (1.40)	0.10	0.79
Attention, mean (SD)	0.04 (1.19)	-0.69 (1.20)	<0.001	0.02
Language, mean (SD)	0.09 (1.14)	-0.69 (1.27)	<0.001	0.002
Visual-spatial, mean (SD)	0.36 (1.02)	-0.02 (1.22)	0.02	0.28

Abbreviations: CDD = CSF dynamics disorder; HCTS = high-convexity tight sulci.

<sup>a</sup> For cognitive tests, raw test scores were averaged and scaled to create a domain z score. The z scores from the 4 domains were averaged and scaled to calculate a global cognitive z score.

<sup>b</sup> Adjusted for age and sex.

cortical thickness could not be explained by focal sulcal effacement. This finding also indicates that HCTS represents a subpopulation of individuals who would be labeled suspected non-Alzheimer pathology by biomarkers.<sup>25</sup> Because biomarkers are increasingly used to determine eligibility in clinical trials and to measure outcomes, it is important to recognize the HCTS pattern of cortical anatomy. For example, if a clinical trial aims to enroll cognitively normal individuals and includes a neurodegeneration biomarker, amyloid-positive individuals with a CDD may be erroneously enrolled, which may affect interpretation of the results. Those with HCTS were less likely to be T+. A possible explanation for this observation is that individuals with significant AD pathology (i.e., A + T + N+) will not have an HCTS because the sulci will be widened due to generalized neurodegenerative brain atrophy.

HCTS and idiopathic NPH are both felt to be manifestations of CDDs. NPH manifests with gait impairment, cognitive impairment, and urinary incontinence; these symptoms improve with a CSF-diverting shunt. In fact, the presence of high-convexity tightness is included in Japanese guidelines for the management of idiopathic NPH.<sup>26</sup> Although the presence of HCTS is an established prognostic feature in patients who also have NPH, HCTS is also observed in the general population. Unlike ventriculomegaly and enlarged Sylvian fissures, which can occur with both neurodegenerative atrophy and CDDs, HCTS does not occur as a consequence of neurodegenerative disease, which is why it was the focus of the current analysis. The limitation of this approach is that it may underestimate the frequency of other manifestations of CDDs (e.g., focal sulcal dilation reflecting extraventricular hydrocephalus) not captured by the current approach.<sup>27</sup>

Recent population-based studies have shown that the neuroimaging features associated with the clinical phenotype of NPH are more common in the general population than previously recognized. For example, a Swedish study of persons >80 years of age showed that 5.4% of the population had HCTS (the term used in that study was occluded sulci).<sup>3</sup> In

a community-based Japanese study, ≈2.9% of elderly individuals had ventriculomegaly with high-convexity tightness.<sup>3</sup> Longitudinal studies will determine whether individuals with HCTS in the general population represent a prodromal variant or an early imaging manifestation of NPH. The link between NPH and HCTS suggests that HCTS also represents a disorder of CSF dynamics, but the pathophysiology of HCTS remains uncertain at this time.

We observed no significant differences in gait velocity between the groups in our study, and currently, gait is the only feature of NPH reliably treated with shunt surgery. Whether gait differences between these 2 groups appear over time is an important area for future investigations.

The HCTS group had more neuroimaging characteristics consistent with vascular disease than the non-HCTS group. This difference was not surprising because individuals with neuroimaging features of NPH have increased white matter hyperintensity volume suggestive of extravasation of CSF, as well as an increased frequency of subcortical infarcts. Vascular risk factors may have a role in the development of hydrocephalus.<sup>28</sup>

CSF AD biomarkers are currently used interchangeably with amyloid and tau PET in the recent AD research criteria.<sup>7</sup> However, unlike imaging, CSF biomarkers are susceptible to confounding with CDDs. In AD,  $\beta$ -amyloid<sub>42</sub> ( $A\beta_{42}$ ) is low in the CSF, whereas total tau and phosphorylated tau are elevated. In NPH, however, many proteins, including  $A\beta_{42}$ , total tau, and phosphorylated tau, are low, with protein levels normalizing after a shunt.<sup>29</sup> The finding of low  $A\beta_{42}$  and tau in NPH has been confirmed in several studies.<sup>30,31</sup> Because  $A\beta_{42}$  is low in NPH and AD, the utility of CSF biomarkers is limited for distinguishing AD from NPH. Moreover, individuals with imaging features of CDD may have low  $A\beta_{42}$  and tau, which can cause discrepant CSF and amyloid PET values. For example, an individual who was amyloid negative by PET may appear amyloid positive by CSF in the presence of a CDD because the  $A\beta_{42}$  in the CSF is low.

HCTS has been underrecognized as a contributor to biomarker abnormalities for several reasons. First, the association of high-convexity tightness with enlarged Sylvian fissures and parieto-occipital fissures is not recognized and is frequently mistaken as degenerative atrophy. Second, HCTS and DESH are detectable in vivo only. Therefore, pathologic studies cannot be used to investigate this phenomenon. Third, as research datasets increase in size, visual assessment of all scans becomes logistically impractical.

Strengths of this study include the large number of population-sampled participants, the use of automated MRI- and PET-based imaging biomarkers of AD, and our in-house automated HCTS classifier. The study has limitations, including that HCTS is an indirect marker of disturbed CSF dynamics. While HCTS was described in a subset of patients with NPH and is a predictor of shunt responsiveness,<sup>6</sup> because it is an indirect marker of a CDD, it is possible that not all patients with an HCTS have a CDD. While the focus of this study was on AD PET biomarkers, because there can be a dissociation between AD PET and CSF biomarkers, future studies should determine whether those with HCTS are overrepresented in discrepant cases. Current tau PET ligands such AV-1451 have limited use in non-AD tauopathies; therefore, we cannot exclude that pathologies not measured by tau PET such as 4 R tau and TAR DNA-binding protein 43 were not present in the cases with HCTS. Future studies evaluating CSF flow directly or with neuroimaging will be important in confirming the findings of this study. Our current algorithm detects HCTS only; therefore, we likely underestimated the total impact of the commonly associated ventricular enlargement and sulcal widening elsewhere.

Although individuals with neuroimaging features consistent with HCTS are uncommon in the general population, the features of HCTS should be better characterized because they appear to have distinct clinical effects (i.e., cognitive impairment) and are associated with AD biomarkers. The longitudinal clinical implications of these biomarkers need to be studied.

Acknowledgment

The authors thank AVID Radiopharmaceuticals, Inc for supplying the AV-1451 precursor, chemistry production advice, and oversight, as well as the US Food and Drug Administration regulatory cross-filing permission and documentation needed for this work.

Study funding

Funded by the NIH: K76 AG057015 (J. Graff-Radford), R37 AG011378 (Jack), R01 AG041851 (Jack and Knopman), U01 AG006786 (Petersen; MCSA), R01 NS097495 (Vemuri), and P50 AG016574 (Petersen). Other sources include the Elsie and Marvin Dekelboum Family Foundation, Alexander Family Professor of Alzheimer’s Disease Research, Mayo Clinic, Liston Award, Schuler Foundation, GHR Foundation, and Mayo Foundation for Medical Education and Research. This study was made possible by the resources of the Rochester Epidemiology Project, which is supported by the National Institute

on Aging of the NIH under award R01AG034676. The content is solely the responsibility of the authors and does not necessarily represent the official views of the NIH.

Disclosure

J. Graff-Radford receives research funding from National Institute on Aging/NIH. J. Gunter, D. Jones, S. Przybelski, and C. Schwarz report no disclosures relevant to the manuscript. J. Huston reports patents from the Mayo Foundation, royalties from Resoundant stock, and stock options in Resoundant. V. Lowe serves on scientific advisory boards for Bayer Schering Pharma, Piramal Life Sciences, and Merck Research and receives research support from GE Healthcare, Siemens Molecular Imaging, AVID Radiopharmaceuticals, and NIH (National Institute on Aging, National Cancer Institute). B. Elder reports no disclosures relevant to the manuscript. M. Machulda receives NIH funding. N. Gunter reports no disclosures relevant to the manuscript. R. Petersen is a consultant for Roche, Biogen, Merck, Eli Lilly, and Genentech. He receives publishing royalties from *Mild Cognitive Impairment* (Oxford University Press, 2003) and research support from NIH. K. Kantarci serves on the data safety monitoring board for Takeda Global Research & Development Center, Inc and receives research support from the NIH. P. Vemuri receives NIH funding. M. Mielke is a consultant for Eli Lilly and Lysosomal Therapeutics and receives unrestricted research grants from Biogen, Lundbeck, and Roche and research funding from NIH/National Institute on Aging and the US Department of Defense. D. Knopman serves on a data safety monitoring board for the Dominantly Inherited Alzheimer’s Disease study. He is an investigator in clinical trials sponsored by Lilly Pharmaceuticals, Biogen, and the Alzheimer’s Treatment and Research Institute at the University of Southern California and receives research support from NIH. N. Graff-Radford serves on a scientific advisory board for Codman; serves on the editorial boards of *The Neurologist* and *Alzheimer’s Research & Therapy*; has received publishing royalties from UpToDate; and receives research support from Biogen, Lilly, and Axovant. He has consulted for Cytex. C. Jack consults for Lily and serves on an independent data monitoring board for Roche. He receives research support from NIH/National Institute on Aging and the Alexander Family Professor of Alzheimer’s Disease Research, Mayo Clinic. Go to [Neurology.org/N](http://Neurology.org/N) for full disclosures.

Publication history

Received by *Neurology* February 12, 2019. Accepted in final form June 19, 2019.

Appendix Authors

Name	Location	Role	Contribution
Jonathan Graff-Radford, MD	Department of Neurology, Mayo Clinic, Rochester, MN	Author	Study concept and design, data interpretation, drafting the original report, obtaining funding



## Appendix (continued)

Name	Location	Role	Contribution
<b>Jeffrey L. Gunter, PhD</b>	Department of Radiology, Mayo Clinic, Rochester, MN	Author	Data collection and analyses, critical revision of the manuscript
<b>David T. Jones, MD</b>	Department of Neurology, Mayo Clinic, Rochester, MN	Author	Data collection and analyses, critical revision of the manuscript
<b>Scott A. Przybelski</b>	Department of Health Sciences Research, Mayo Clinic, Rochester, MN	Author	Data collection and analyses, statistical analysis, critical revision of the manuscript
<b>Christopher G. Schwarz, PhD</b>	Department of Radiology, Mayo Clinic, Rochester, MN	Author	Data collection and analyses, critical revision of the manuscript
<b>John Huston III, MD</b>	Department of Radiology, Mayo Clinic, Rochester, MN	Author	Data collection and analyses, critical revision of the manuscript
<b>Val Lowe, MD</b>	Department of Radiology, Mayo Clinic, Rochester, MN	Author	Data collection and analyses, critical revision of the manuscript
<b>Benjamin D. Elder, MD, PhD</b>	Department of Neurosurgery, Mayo Clinic, Rochester, MN	Author	Data collection and analyses, critical revision of the manuscript
<b>Mary M. Machulda, PhD, LP</b>	Department of Psychiatry and Psychology, Mayo Clinic, Rochester, MN	Author	Data collection and analyses, critical revision of the manuscript
<b>Nathaniel B. Gunter</b>	Department of Radiology, Mayo Clinic, Rochester, MN	Author	Data collection and analyses, critical revision of the manuscript
<b>Ronald C. Petersen, MD, PhD</b>	Department of Neurology, Mayo Clinic, Rochester, MN	Author	Data collection and analyses, critical revision of the manuscript, obtaining funding
<b>Kejal Kantarci, MD</b>	Department of Radiology, Mayo Clinic, Rochester, MN	Author	Data collection and analyses, critical revision of the manuscript
<b>Prashanthi Vemuri, PhD</b>	Department of Radiology, Mayo Clinic, Rochester, MN	Author	Data collection and analyses, critical revision of the manuscript, obtaining funding
<b>Michelle M. Mielke, PhD</b>	Department of Health Sciences Research, Mayo Clinic, Rochester, MN	Author	Data collection and analyses, statistical analysis, critical revision of the manuscript
<b>David S. Knopman, MD</b>	Department of Neurology, Mayo Clinic, Rochester, MN	Author	Data collection and analyses, critical revision of the manuscript

## Appendix (continued)

Name	Location	Role	Contribution
<b>Neill R. Graff-Radford, MD</b>	Neurology, Mayo Clinic, Jacksonville, FL	Author	Data collection and analyses, critical revision of the manuscript
<b>Clifford R. Jack, MD</b>	Radiology, Mayo Clinic, Rochester, MN	Author	Study concept and design, data interpretation, and drafting the original report, obtaining funding

## References

1. Hashimoto M, Ishikawa M, Mori E, Kuwana N. Study of INPH on Neurological Improvement (SINPHONI). Diagnosis of idiopathic normal pressure hydrocephalus is supported by MRI-based scheme: a prospective cohort study. *Cerebrospinal Fluid Res* 2010;7:18.
2. Hiraoka K, Meguro K, Mori E. Prevalence of idiopathic normal-pressure hydrocephalus in the elderly population of a Japanese rural community. *Neurol Med Chir (Tokyo)* 2008;48:197–199.
3. Jaraj D, Rabiei K, Marlow T, Jensen C, Skoog I, Wikkelsø C. Prevalence of idiopathic normal-pressure hydrocephalus. *Neurology* 2014;82:1449–1454.
4. Gunter NB, Schwarz CG, Graff-Radford J, et al. Automated detection of imaging features of disproportionately enlarged subarachnoid space hydrocephalus using machine learning methods. *Neuroimage Clin* 2019;21:101605.
5. Yamashita F, Sasaki M, Saito M, et al. Voxel-based morphometry of disproportionate cerebrospinal fluid space distribution for the differential diagnosis of idiopathic normal pressure hydrocephalus. *J Neuroimaging* 2014;24:359–365.
6. Narita W, Nishio Y, Baba T, et al. High-convexity tightness predicts the shunt response in idiopathic normal pressure hydrocephalus. *AJNR Am J Neuroradiol* 2016; 37:1831–1837.
7. Jack CR Jr, Bennett DA, Blennow K, et al. NIA-AA research framework: toward a biological definition of Alzheimer's disease. *Alzheimers Dement* 2018;14:535–562.
8. Roberts RO, Geda YE, Knopman DS, et al. The Mayo Clinic Study of Aging: design and sampling, participation, baseline measures and sample characteristics. *Neuroepidemiology* 2008;30:58–69.
9. St Sauver JL, Grossardt BR, Yawn BP, et al. Data resource profile: the Rochester Epidemiology Project (REP) medical records-linkage system. *Int J Epidemiol* 2012; 41:1614–1624.
10. McKhann GM, Knopman DS, Chertkow H, et al. The diagnosis of dementia due to Alzheimer's disease: recommendations from the National Institute on Aging-Alzheimer's Association workgroups on diagnostic guidelines for Alzheimer's disease. *Alzheimers Dement* 2011;7:263–269.
11. Petersen RC. Mild cognitive impairment as a diagnostic entity. *J Intern Med* 2004; 256:183–194.
12. Mielke MM, Roberts RO, Savica R, et al. Assessing the temporal relationship between cognition and gait: slow gait predicts cognitive decline in the Mayo Clinic Study of Aging. *J Gerontol A Biol Sci Med Sci* 2013;68:929–937.
13. Jack CR Jr, Bernstein MA, Fox NC, et al. The Alzheimer's Disease Neuroimaging Initiative (ADNI): MRI methods. *J Magn Reson Imaging* 2008;27:685–691.
14. Fatemi F, Kantarci K, Graff-Radford J, et al. Sex differences in cerebrovascular pathologies on FLAIR in cognitively unimpaired elderly. *Neurology* 2018;90:e466–e473.
15. Raz L, Jayachandran M, Tosakulwong N, et al. Thrombogenic microvesicles and white matter hyperintensities in postmenopausal women. *Neurology* 2013;80:911–918.
16. Schwarz CG, Gunter JL, Ward CP, et al. The Mayo clinic adult life span template: better quantification across the life span. *Alzheimers Dement* 2017;13:P93–P94.
17. Avants BB, Epstein CL, Grossman M, Gee JC. Symmetric diffeomorphic image registration with cross-correlation: evaluating automated labeling of elderly and neurodegenerative brain. *Med Image Anal* 2008;12:26–41.
18. Fischl B. Freesurfer. *Neuroimage* 2012;62:774–781.
19. Schwarz CG, Gunter JL, Wiste HJ, et al. A large-scale comparison of cortical thickness and volume methods for measuring Alzheimer's disease severity. *Neuroimage Clin* 2016;11:802–812.
20. Jack CR Jr, Lowe VJ, Senjem ML, et al. 11C PiB and structural MRI provide complementary information in imaging of Alzheimer's disease and amnesic mild cognitive impairment. *Brain* 2008;131:665–680.
21. Knopman DS, Jack CR Jr, Wiste HJ, et al. Short-term clinical outcomes for stages of NIA-AA preclinical Alzheimer disease. *Neurology* 2012;78:1576–1582.
22. Jack CR Jr, Wiste HJ, Weigand SD, et al. Defining imaging biomarker cut points for brain aging and Alzheimer's disease. *Alzheimers Dementia* 2017;13: 205–216.

23. Jack CR Jr, Wiste HJ, Weigand SD, et al. Age-specific and sex-specific prevalence of cerebral beta-amyloidosis, tauopathy, and neurodegeneration in cognitively unimpaired individuals aged 50-95 years: a cross-sectional study. *Lancet Neurol* 2017; 16:435–444.
24. von Elm E, Altman DG, Egger M, Pocock SJ, Gøtzsche PC, Vandenbroucke JP. The Strengthening of Reporting of Observational Studies in Epidemiology (STROBE) statement: guidelines for reporting observational studies. *J Clin Epidemiol* 2008;61: 344–349.
25. Jack CR Jr, Knopman DS, Chetelat G, et al. Suspected non-Alzheimer disease pathophysiology: concept and controversy. *Nat Rev Neurol* 2016;12:117–124.
26. Mori E, Ishikawa M, Kato T, et al. Guidelines for management of idiopathic normal pressure hydrocephalus: second edition. *Neurol Med Chir (Tokyo)* 2012;52:775–809.
27. Holodny AI, George AE, de Leon MJ, Golomb J, Kalnin AJ, Cooper PR. Focal dilation and paradoxical collapse of cortical fissures and sulci in patients with normal-pressure hydrocephalus. *J Neurosurg* 1998;89:742–747.
28. Jaraj D, Agerskov S, Rabiei K, et al. Vascular factors in suspected normal pressure hydrocephalus: a population-based study. *Neurology* 2016;86:592–599.
29. Jeppsson A, Zetterberg H, Blennow K, Wikkelso C. Idiopathic normal-pressure hydrocephalus: pathophysiology and diagnosis by CSF biomarkers. *Neurology* 2013;80:1385–1392.
30. Graff-Radford NR. Alzheimer CSF biomarkers may be misleading in normal-pressure hydrocephalus. *Neurology* 2014;83:1573–1575.
31. Kapaki EN, Paraskevas GP, Tzerakis NG, et al. Cerebrospinal fluid tau, phospho-tau181 and beta-amyloid1-42 in idiopathic normal pressure hydrocephalus: a discrimination from Alzheimer's disease. *Eur J Neurol* 2007;14:168–173.

# Neurology®

## Cerebrospinal fluid dynamics disorders: Relationship to Alzheimer biomarkers and cognition

Jonathan Graff-Radford, Jeffrey L. Gunter, David T. Jones, et al.

*Neurology* published online November 12, 2019

DOI 10.1212/WNL.00000000000008616

**This information is current as of November 12, 2019**

### Updated Information & Services

including high resolution figures, can be found at:  
<http://n.neurology.org/content/early/2019/11/11/WNL.00000000000008616.full>

### Subspecialty Collections

This article, along with others on similar topics, appears in the following collection(s):  
**Alzheimer's disease**  
[http://n.neurology.org/cgi/collection/alzheimers\\_disease](http://n.neurology.org/cgi/collection/alzheimers_disease)

### Permissions & Licensing

Information about reproducing this article in parts (figures, tables) or in its entirety can be found online at:  
[http://www.neurology.org/about/about\\_the\\_journal#permissions](http://www.neurology.org/about/about_the_journal#permissions)

### Reprints

Information about ordering reprints can be found online:  
<http://n.neurology.org/subscribers/advertise>

*Neurology*® is the official journal of the American Academy of Neurology. Published continuously since 1951, it is now a weekly with 48 issues per year. Copyright © 2019 American Academy of Neurology. All rights reserved. Print ISSN: 0028-3878. Online ISSN: 1526-632X.

